CHAPTER 13

Insights into the Pore of the Hair Cell Transducer Channel from Experiments with Permeant Blockers

Sietse M. van Netten* **and Corné J. Kros**[†]

*Department of Neurobiophysics, University of Groningen, 9747AG, Groningen, The Netherlands

[†]School of Life Sciences, University of Sussex, Falmer, Brighton BN1 9QG, United Kingdom

Current Topics in Membranes, Volume 59
1063-5823/07 $35.00

DOI: 10.1016/S1063-5823(06)59013-1

I. OVERVIEW

This chapter considers recent experiments designed to infer properties of the ion-conducting pore of the mechanoelectrical transducer channel of sensory hair cells using permeant blockers. By combining results from experiments with three classes of large cationic permeant blockers, the fluorescent dye FM1-43, the aminoglycoside antibiotics, and the potassium-sparing diuretic amiloride, information has been obtained on the free energy profile along the transducer channel's pore as sensed by these blocker molecules. These energy profiles provide information about the position of the negatively charged binding site for the blockers (likely to be the channel's selectivity filter) as well as about positively charged barriers near the extracellular and intracellular faces of the channel that impede the blockers' permeation. The extracellular barrier is relatively modest and allows almost diffusion-limited entry of blockers from the extracellular side. A larger intracellular energy barrier effectively prevents exit of the blocking molecules from the intracellular side, trapping the blockers inside the hair cells. A putative geometrical model of the transducer channel pore is presented that draws on results from all three classes of permeant blockers. The pore contains a large vestibule that is easily accessible from the extracellular side. The negatively charged selectivity filter is located at the end of the vestibule, about 2 nm inside the pore from the extracellular side, with the total pore length estimated as 3 nm. Further experiments with permeant blockers may help toward understanding the molecular nature of the hair cell transducer channel and its relation with mechanoreceptor channels in other sensory systems.

II. INTRODUCTION

The molecular identity of the hair cell transducer channel is, despite intensive research efforts, still in question at the time of writing (Corey, 2006). Nevertheless, recent pharmacological characterization is beginning to yield information about key properties of the channel that may help toward its eventual molecular identification by comparison with other known channel types. Historically, the pharmacology of the transducer channel has been studied to try and find the mode of action of ototoxic drugs. Particularly for the widely used aminoglycoside antibiotics, large polycationic molecules which lead to permanent hearing loss (reviewed by Forge and Schacht, 2000) associated with hair cell degeneration (Wersäll *et al.*, 1973), the transducer channel has been implicated early on as a possible target. This is because aminoglycosides were found to block extracellularly recorded electrical responses when administered into the endolymph (into which the hair bundles

that contain the transducer channels protrude) but not the perilymph (which surrounds the basolateral membrane of the hair cells), both in the goldfish sacculus (Matsuura *et al.*, 1971) and the guinea pig cochlea (Konishi, 1979).

The first studies in which the effects of aminoglycoside antibiotics were tested directly on the responses of individual hair cells showed that the drugs blocked the transducer channel from the extracellular but not the intracellular side (Ohmori, 1985; Kroese *et al.*, 1989). What remained puzzling was how the drug molecules might enter the hair cells where they are believed to exert their ototoxic effects (Schacht, 1986; Hiel *et al.*, 1993). The possibility that the transducer channels might be slightly permeable to aminoglycosides was considered but thought unlikely. This was because at the time the diameter of the transducer channel pore was estimated as about 0.7 nm, based on its finite permeability to the ion channel blocker tetraethylammonium (TEA; Ohmori, 1985; Howard *et al.*, 1988). The minimal diameter of a number of different aminoglycoside antibiotics was estimated as about 1 nm. It was therefore considered uncertain at the time whether the channel block was a necessary step in the chain of events leading to ototoxicity (Kroese *et al.*, 1989). Experiments with a large number of blockers, however, have led to a revision of the minimum pore size of the transducer channel to about 1.25 nm (Farris *et al.*, 2004). Following on from the discovery that an unrelated large polycationic molecule, the styryl dye FM1-43, permeates through the transducer channel (Gale *et al.*, 2001), aminoglycoside block was reexamined, leading to the conclusion that these drugs also can enter the hair cells through the transducer channel after all (Marcotti *et al.*, 2005). In this chapter, we will discuss experiments with a variety of permeant blockers and the insights these experiments provide into the pore structure of the transducer channel and its relation to other ion channel types.

III. IONIC SELECTIVITY OF THE TRANSDUCER CHANNEL

The hair cell transducer channel is a nonselective cation channel with very similar permeabilities for the alkali cations and a much higher permeability for divalent metal ions, the highest for Ca^{2+} (Ohmori, 1985; Jorgensen and Kroese, 1995). The permeability sequence of the alkali metal ions corresponds to Eisenman sequence XI, pointing to a high negative charge density of the selectivity filter (Hille, 2001). The high affinity of the Ca^{2+} ions for the selectivity filter has the effect that Ca^{2+}, although more permeable, has a lower conductance than monovalent metal cations. The Ca^{2+} ions thus tend to linger around in the pore and act as permeant blockers of the transducer current with a half-blocking concentration (K_D) of about 1 mM and a Hill coefficient of 1 (Crawford *et al.*, 1991; Ricci and Fettiplace, 1998;

Fettiplace and Ricci, 2006). Due to the composition of the endolymph (high K^+, micromolar Ca^{2+}) most of the transducer current is *in vivo* carried by K^+ ions, with the Ca^{2+} concentration optimized to ensure a large transducer current with sufficient Ca^{2+} entering to drive adaptation (Ricci and Fettiplace, 1998). The current–voltage curves of transducer currents of mammalian outer hair cells (OHCs) in the presence of 1.3-mM extracellular Ca^{2+} show inward rectification at negative potentials and outward rectification at positive potentials. This double rectification is compatible with Ca^{2+} acting as a permeant blocker that is dislodged from its binding site and extruded from the channel at extreme potentials (Kros *et al.*, 1992; Kros, 1996). The simplest quantitative model that fits these observations (a single energy barrier formed by bound Ca^{2+} ions that impedes flow of monovalent cations) suggests that the binding site for Ca^{2+} is situated at an electrical distance about halfway through the pore (Kros *et al.*, 1992).

IV. PERMEATION AND BLOCK OF MECHANORECEPTOR CHANNELS BY FM1-43

A. Evidence for Permeation of FM1-43 Through the Hair Cell Transducer Channel

FM1-43 (Fig. 1) is a fluorescent styryl dye with a divalent cationic head group related to TEA and a long lipophilic tail which enables it to partition reversibly into the outer leaflet of the cell membrane when present in the extracellular solution (Betz *et al.*, 1992). On incorporation into the membrane, its fluorescence increases by two orders of magnitude. It cannot cross the lipid bilayer so that when it becomes internalized into cells by endocytosis, it remains trapped in the inner leaflet of endocytosed vesicles, the basis for its use as a tracker of endo- and exocytosis in living cells (Betz and Bewick, 1992; Cochilla *et al.*, 1999). The dye readily labels sensory hair cells from their apical surface, leading to the conclusion that a rapid endocytotic process operates in their apical region (Seiler and Nicolson, 1999). However, a number of observations did not easily fit with this interpretation. Aminoglycosides and amiloride (also a transducer channel blocker; see Section VI.A) as well as high concentrations of extracellular Ca^{2+} inhibited dye labeling of hair cells in the *Xenopus* lateral line, leading to the suggestion that the dye might enter through the transducer channels instead (Nishikawa and Sasaki, 1996). These findings were confirmed and extended in the mammalian cochlea in which confocal microscopy showed rapid FM1-43 entry in inner hair cells (IHCs) and OHCs (but not nearby supporting cells) from the apical surface (Gale *et al.*, 2001). FM1-43 loading was prevented by

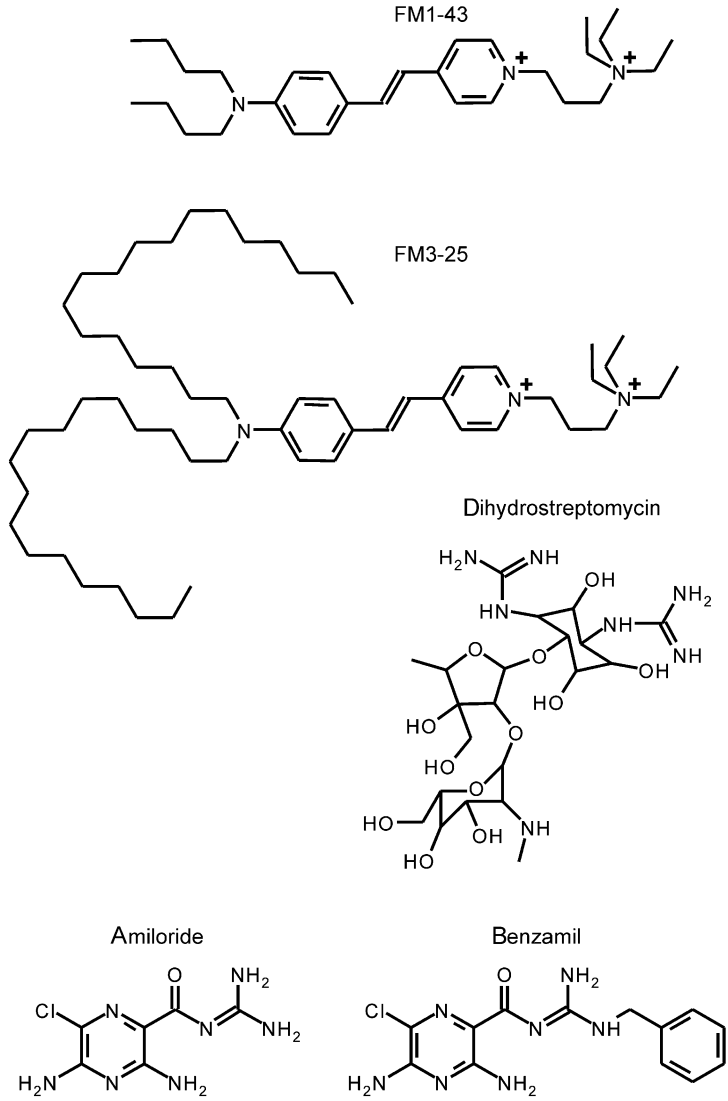

FIGURE 1 Structure of five permeant blocker molecules of the mechanoelectrical transducer channel, as discussed and compared in this chapter. The styryl dyes FM1-43 and FM3-25 are related in that the two butyl end groups of the lipophilic tail in FM1-43 are replaced by two octadecyl groups in FM3-25 giving it the appearance of a fishhook. The aminoglycoside antibiotic dihydrostreptomycin has the largest end-on diameter of the five molecules shown, while the potassium-sparing diuretics amiloride and its analogue benzamil are the smallest molecules.

pretreatment with a high concentration of the Ca^{2+} chelator EGTA, which would abolish transducer currents by cutting the tip links that gate the transducer channels (Crawford *et al.*, 1991). Dye loading recovered with time hours after EGTA was removed, suggesting tip links regenerated over time (Zhao *et al.*, 1996). The degree of FM1-43 loading was larger in OHCs than in adjacent IHCs and larger in hair cells located more basally along the cochlear coils, thus showing correlation with the expected size of the (resting) transducer current (Kros *et al.*, 1992; Kros, 1996; He *et al.*, 2004).

The most direct evidence for entry of FM1-43 through the transducer channel came from recordings of transducer currents (Gale *et al.*, 2001, replotted in Fig. 2). FM1-43 blocked transducer currents in a voltage-dependent manner, such that the block was maximal at intermediate and reduced at extreme negative and positive membrane potentials. The current-voltage curves in the presence of FM1-43 were in effect exaggerated versions of the double rectification attributed to Ca^{2+} ions acting as permeant blockers of the transducer channel (Kros *et al.*, 1992). The rectification was much steeper in the presence of FM1-43, but the barrier for permeation of monovalent ions was about halfway through the transducer channel, just as for Ca^{2+}. The K_D of FM1-43 block was three orders of magnitude lower than that of Ca^{2+}, at 1-3 μM (obviously varying with membrane potential) in the presence of 1.3-mM extracellular Ca^{2+}, making it the most potent transducer channel blocker known to date (Gale *et al.*, 2001; Farris *et al.*, 2004).

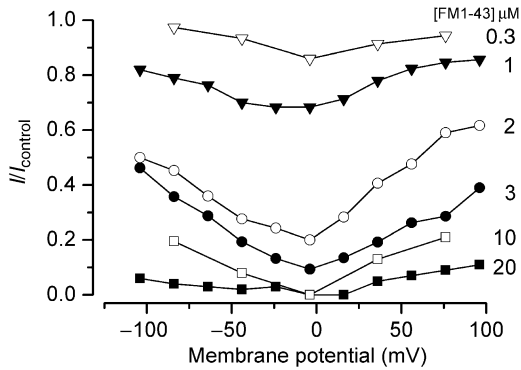

FIGURE 2 Block of mechanoelectrical transducer currents in mouse OHCs by extracellularly applied FM1-43. Data are from Gale *et al.* (2001), with permission, but blocked current is plotted here as a fraction of the control current. The voltage dependence of the block, in the presence of 1.3-mM extracellular Ca^{2+}, is shown for different extracellular concentrations ranging from 0.3 to 20 μM, as indicated on the right-hand side of each trace. The blockage is most pronounced at membrane potentials close to zero and reduces at both hyperpolarizing and depolarizing membrane potentials, the former is evidence of permeation through the channel (Section IV.A). Copyright (2001) by the Society for Neuroscience.

FM1-43 block was even more effective when extracellular Ca^{2+} was lowered to 100 μM and much less so in 10-mM Ca^{2+}. The Hill coefficient was around 2 at intermediate potentials, reducing to near 1 at extreme negative and positive potentials, pointing to possible ionic interactions in the pore. Overall, these findings suggest that FM1-43 competes with Ca^{2+} for a minimum of two binding sites about halfway through the pore of the transducer channel. When applied intracellularly, even 50-μM FM1-43 did not block the transducer currents at any potential, despite the low intracellular free Ca^{2+} concentration. This shows that FM1-43 passes the channel preferentially in one direction, enabling the drug to accumulate in the hair cells.

The kinetics of FM1-43 block suggest that the drug molecules may be trapped inside the closed channel (Gale *et al.*, 2001). FM1-43 is an elongated molecule with a maximum end-on diameter of about 0.78 nm and a length of about 2.2 nm, putting a minimum of about 0.8 nm on the size of the selectivity filter and suggesting a vestibule facing the extracellular side of the channel that is sufficiently large to accommodate at least two FM1-43 molecules. FM3-25 is a derivative of FM1-43 in which the two butyl end groups of the lipophilic tail (at the opposite end of the molecule to the divalent cationic head group) are replaced by two much longer octadecyl groups (Fig. 1). This increase from 4 to 18 carbons gives FM3-25 a shape rather like a fishhook (Meyers *et al.*, 2003), which would limit the depth to which the head group can penetrate the transducer channel pore to about 1.8 nm. FM3-25 dye did not enter the hair cells or block the transducer current at any concentration tested (up to 30 μM). This suggests that the FM3-25 cationic head group was unable to reach its binding site inside the channel pore, putting a lower limit of a distance of 1.8 nm into the pore on the position of the binding site, which may well be the selectivity filter.

B. Permeation of FM1-43 Through Other Mechanoreceptors

Using cell lines transfected with various ion channels, FM1-43 dye has been demonstrated to permeate through TRPV1 channels when activated by capsaicin or heat, and through $P2X_2$ purinoreceptors activated by ATP (Meyers *et al.*, 2003). This is a useful observation as finding molecularly characterized ion channel types with structural similarities to the hair cell transducer channel may help with the search for its molecular identity. When injected into living mice, FM1-43 was moreover able to label many different types of sensory cells throughout the body, while not labeling nonsensory cells (Meyers *et al.*, 2003). It is possible that FM1-43 may have entered these cell types through their sensory transducer channels, again opening

up new ways to put the hair cell mechanoelectrical transducer channel in context.

C. *FM1-43 as a Screen for Functional Transducer Channels and Mechanoreceptors*

As FM1-43 requires transducer channels to be open for it to label hair cells and probably other sensory cells, it provides a rapid and convenient optical means to screen for the proper function of these channels. For example, mutations in the gene encoding the unconventional myosin, myosin VIIA, lead to deafness in humans and shaker1 mice. The hair bundles of *Myo7a* mutant mice need to be displaced beyond their physiological operating range for the transducer channels to open and they hyperadapt to excitatory stimuli (Kros *et al*., 2002). This points to a role for myosin VIIA in anchoring membrane proteins to the actin core of the stereocilia. The lack of transducer channels open at rest (normally 5–10%) in homozygous *Myo7a* mutant mice prevents FM1-43 loading of the hair cells and labeling was only restored when the hair bundles were stimulated by large excitatory force steps (Gale *et al*., 2001). FM1-43 could thus be used as a screen for mutations affecting hair cell transduction. Other applications that have been used include screening for the onset during development of mechanoelectrical transduction by hair cells (Géléoc and Holt, 2003; Si *et al*., 2003) and monitoring the recovery of hair cell function following ototoxic damage by aminoglycoside antibiotics (Taura *et al*., 2006).

V. PERMEATION AND BLOCK OF THE HAIR CELL TRANSDUCER CHANNEL BY AMINOGLYCOSIDE ANTIBIOTICS

A. *Evidence for Permeation of Aminoglycoside Antibiotics Through the Transducer Channel*

The studies of Ohmori (1985) and Kroese *et al*. (1989) showed that extracellularly applied aminoglycoside antibiotics reversibly blocked transducer currents at negative but not at positive potentials. Kroese *et al*. (1989) also found that intracellularly applied aminoglycosides did not block the transducer currents even at concentrations of 500 μM, one to two orders of magnitude higher than the concentrations with which they achieved block from the extracellular side. The K_D for extracellularly applied aminoglycosides increased when the extracellular Ca^{2+} concentration was increased, pointing to competition between the two ions. Aminoglycoside block was

quantitatively interpreted as an interaction with a binding site inside the transducer channel, reachable only from the extracellular side, that blocks the flow of cations through the channel at negative potentials (Kroese *et al.*, 1989). The Hill coefficient was 1, implying that an interaction of one aminoglycoside molecule with the binding site is sufficient to block monovalent cation current through the channel. Assuming two positive charges for the aminoglycoside dihydrostreptomycin (DHS; see Fig. 1 for its structure), the binding site was estimated to be at an electrical distance of 20% into the channel from its extracellular side.

Experiments by Marcotti *et al.* (2005) provided several advances over these early studies. By extending the range of membrane potentials used to voltage clamp individual hair cells, it became evident that block of the transducer current by extracellular DHS became progressively reduced at large negative potentials beyond −80 mV (Fig. 3). This could be explained if the blocking site was cleared due to the drug molecules being dragged through the channel pore into the cells by the large electrical driving force, in other words, if DHS acted as a permeant channel blocker like FM1-43. Intracellular DHS, when tested at extremely high concentrations (up to 10 mM) and over a larger range of membrane potentials than before, was found to block the transducer current, but now at positive potentials, so with opposite polarity to

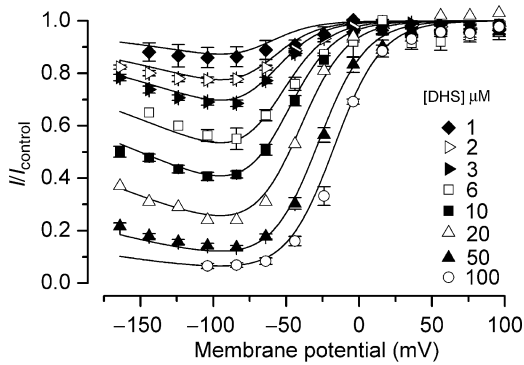

FIGURE 3 Mechanoelectrical transducer currents in mouse OHCs blocked by extracellularly applied DHS and depicted as a fraction of control currents (from Marcotti *et al.*, 2005, with permission). The voltage dependence of the block, in the presence of 1.3-mM extracellular Ca^{2+}, is shown for different extracellular concentrations ranging from 1 to 100 μM DHS, as indicated with the various symbols. Continuous lines were calculated with the 2B1BS model [Section V.B.1; Eq. (6)]. Parameters used in the model are the same for all concentrations shown: $\Delta E = E_2 - E_1 = 4.63kT$; $\Delta\delta = \delta_2 - \delta_1 = 0.91$; $E_b = -8.27kT$; $\delta_b = 0.79$; $n_H = 1$, and $z = 2$. The reduction of blockage at potentials more negative than about −92 mV [Eq. (8)] signifies an increased permeation of DHS through the channel at these voltages.

extracellular DHS. This indicated that the DHS binding site in the channel could also be reached from the intracellular solution after all, further strengthening the case for DHS being a permeant blocker. The fact that the K_D for intracellular block was two to three orders of magnitude higher than for extracellular block, together with the normally large negative driving force across the transducer channel (about −150 mV) brought about by the endocochlear potential explains why the transducer channel effectively acts as a one-way valve for aminoglycoside antibiotics so that they can accumulate in the hair cells. The kinetics of the block in response to mechanical steps and voltage steps showed that the transducer channel has to open first before DHS block can occur (Marcotti *et al.*, 2005). In contrast to FM1-43, DHS is thus an open channel blocker of the transducer channel. This may be the reason why the efficacy of DHS block is reduced in *Myo7a* mutant mice, which have very low resting open probability of their transducer channels (Kros *et al.*, 2002), and why the K_D for rapidly adapting high-frequency hair cells in the turtle cochlea is higher than for the more slowly adapting low-frequency hair cells (Ricci, 2002). Moreover, the transducer current shuts off more slowly than normal in the presence of DHS, implying that the channel cannot close with the blocker present in the pore. This fits with the reported disappearance of the gating compliance when the transducer channels are blocked by aminoglycosides (Howard and Hudspeth, 1988). This behavior of DHS is again in contrast to FM1-43, which is likely to be able to reside inside the closed channel (Section IV.A). Perhaps this is due to DHS (molecular weight of the free base 583.6) being a somewhat bulkier molecule than FM1-43 (molecular weight 451), with an end-on diameter of about 1 nm and a length of about 1.5 nm. On the other hand, benzamil is smaller than both and also interferes with closure of the channel (Section VI.A), so other factors may be involved. The ability to enter hair cells through their transducer channels is likely to be a general property of aminoglycosides as qualitatively similar observations to those using DHS have been made with neomycin and gentamicin (Kros *et al.*, 2006).

B. *Inferences About the Functional Geometry of the Transducer Channel Pore*

To quantitatively describe the voltage and concentration dependences of blockage and permeation of the hair cell transducer channel by permeant blocker molecules, like DHS, a two-barrier one-binding site (2B1BS) model of the transducer channel will be considered. A similar approach has been utilized previously to describe voltage-dependent proton block (Woodhull, 1973) and has been applied more generally to the binding of ions to, and

permeation through, an ion channel pore (Hille, 2001). An equivalent "punch-through" model was considered for blockage of amiloride and several analogues of mechanosensitive channels in *Xenopus* oocytes, but discarded because the measured behavior at large hyperpolarizing potentials did not suggest permeant block (Lane *et al.*, 1991). The model described here provides a more complete treatment of the 2B1BS model used by Marcotti *et al.* (2005) and introduces two new elements: the possibility to apply the model to blocking interactions with Hill coefficients other than 1 and a quantitative analysis of drug binding from the intracellular side.

The rate constants that are applied in the 2B1BS model description can be determined via Eyring's rate theory applied to the two energy barriers (Fig. 4). This yields results that are equivalent to a stochastic description of diffusion, which can be interpreted as a random hopping of particles, surmounting energy barriers (Hille, 2001). The blocker molecules are

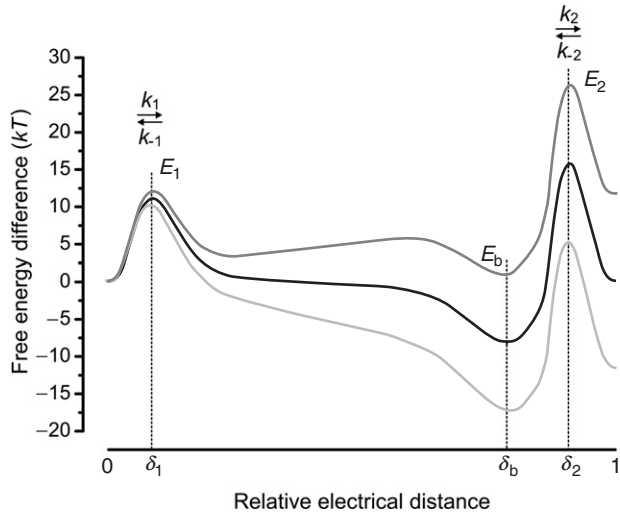

FIGURE 4 Free energy profiles of the 2B1BS model used to describe the voltage and concentration dependent block and permeation of extracellularly applied DHS (Section V) and amiloride (Section VI). The free energy differences are shown for three membrane voltages +150 mV (top, dark gray curve), 0 mV (middle, black curve), and −150 mV (bottom, light gray curve). Changing the membrane voltage effectively tilts the energy profile. The barriers are indicated with E_1 and E_2 and are located at relative electrical distance δ_1 and δ_2, respectively, as measured across the membrane from the extracellular side. The binding site with relative free energy E_b is located at δ_b. The actual values of E_1, E_2, E_b, δ_1, δ_2, and δ_b as shown are the results obtained for DHS at 1.3-mM extracellular Ca^{2+}.

attracted to a preferred position with low free energy which can therefore be considered as the binding site.

Rate constants in Eyring's rate theory depend exponentially on the ratio of Gibbs free energy of the barriers and the thermal energy kT, similar to Arrhenius' equation of chemical reactions in which the rate constants k_r are related to the ratio of activation energy E_A and kT [$k_r \propto \exp(-E_A/(kT))$]. The free energy related to the membrane potential V contributes to E_A and thus causes the rate constants to be voltage dependent. The equilibrium reached will therefore also depend on the membrane potential. In the following sections, we discuss some specific consequences of the 2B1BS model in relation to permeation of blocker molecules.

1. General Model Equations

Assuming that the unblocked transducer channels are indicated by C, the blocked channels by CB, the extra- and intracellular blocker by B_o and B_i, and using the forward (k_1, k_2) and reverse (k_{-1}, k_{-2}) rate constants, the reaction equation is given by:

$$C + B_o \underset{k_{-1}}{\overset{k_1}{\Leftrightarrow}} CB \underset{k_{-2}}{\overset{k_2}{\Leftrightarrow}} C + B_i \tag{1}$$

Experiments showed that DHS is an open channel blocker (Section V.A). In the further discussion below of the reaction equation [Eq. (1)], we assume that the blocker can reach the binding site from the moment that the channels are opened via a mechanical stimulus. Alternatively, the same dynamics may be obtained via a sudden change of the blocker concentration on either the extra- or intracellular side of the membrane or of the membrane voltage. Assigning t to the description of the dynamics as the time variable, $C(t)$ and $CB(t) = 1 - C(t)$ denote the time-dependent fractions of unblocked and blocked channels. The rate of change of $C(t)$ is dependent on the four rate constants k_1, k_{-1}, k_2, and k_{-2} of the transitions across the barriers and the intra- and extracellular blocker concentrations $[B_i]$ and $[B_o]$ according to:

$$\frac{dC(t)}{dt} = (-k_1[B_o]^{n_H} - k_{-2}[B_i]^{n_H}) \cdot C(t) + (k_{-1} + k_2)CB(t) \tag{2}$$

Here, the Hill coefficient n_H is the degree of cooperativity of the binding process of the blocker to the binding site. A general solution of Eq. (2), describing the approach to equilibrium can be written as:

$$C(t) = C(\infty) + [C(0) - C(\infty)]\exp(-t/\tau), \tag{3a}$$

where the time constant τ is given by:

$$\tau = \frac{1}{k_1[B_o]^{n_H} + k_{-2}[B_i]^{n_H} + k_{-1} + k_2} \tag{3b}$$

The steady state or equilibrium solution of Eq. (3a) (reached if, $t \to \infty$, so that $dC(t)/dt = 0$) is then given by:

$$C(\infty) = \tau(k_{-1} + k_2), \tag{4a}$$

which is assumed to equal the ratio of blocked current I to the control (unblocked) current I_c, yielding:

$$\frac{I}{I_c} = C(\infty) = \frac{k_{-1} + k_2}{k_1[B_o]^{n_H} + k_{-2}[B_i]^{n_H} + k_{-1} + k_2} \tag{4b}$$

To incorporate voltage dependence in the model description, the rate constants (k_1, k_2, k_{-1}, and k_{-2}) can be quantified using Eyring's rate theory, and thus expressed as exponential functions of the difference between the free energy of the barrier maxima and the binding site minimum (Hille, 2001). The free energy differences have both a chemical and a voltage-dependent component. The voltage is assumed to vary with a fixed gradient so that it linearly changes the free energy across the membrane, effectively tilting the overall free energy profile depending on the membrane potential V, as illustrated in Fig. 4 for three different membrane potentials. Defining the maxima of the free energy of the barriers as E_1 and E_2 and the free energy of the binding site as E_b, with respect to $V = 0$ (Fig. 4), and denoting their fractional positions across the membrane byδ_1,δ_2, and $\delta_b$the rate constants are:

$$k_1(V) = k_0' \exp\left(-\frac{E_1}{kT} - \frac{\delta_1 V}{V_s}\right) (\text{s mol}^{n_H})^{-1} \tag{5a}$$

$$k_{-1}(V) = k_0 \exp\left(-\frac{E_1 - E_b}{kT} - \frac{(\delta_1 - \delta_b)V}{V_s}\right) s^{-1} \tag{5b}$$

$$k_2(V) = k_0 \exp\left(-\frac{E_2 - E_b}{kT} - \frac{(\delta_2 - \delta_b)V}{V_s}\right) s^{-1} \tag{5c}$$

$$k_{-2}(V) = k_0' \exp\left(-\frac{E_2}{kT} - \frac{(\delta_2 - 1)V}{V_s}\right) (\text{s mol}^{n_H})^{-1} \tag{5d}$$

Here $V_s = \left(\frac{RT}{zF}\right) = \frac{kT}{ze_0}$, where kT (4.1×10^{-21} J) is the thermal noise energy, z the blocker molecule's valence, and e_0 the elementary charge (1.6×10^{-21} C). The proportionality constant k_0 of the first order rate constants k_{-1} and k_2, and

$k_0' = k_0/\text{mol}^{n_H}$ of the second order rate constants k_1 and k_{-2} are related to the thermal noise energy divided by Planck's constant ($h = 6.63 \times 10^{-34}$ J s). This assumes that the transmission coefficient is one ($k_0 = kT/h$; Hille, 2001). Inserting Eq. (5) into Eq. (4b) then yields:

$$\frac{I}{I_c}(V) = \frac{1}{1 + \left(\left([B_o]^{n_H} + K_2(V) \cdot [B_i]^{n_H}\right)/K_1(V)\right)}, \tag{6a}$$

with

$$K_1(V) = \exp\left(\frac{E_b}{kT} + \frac{\delta_b V}{V_s}\right) \cdot \left[1 + \exp\left(-\frac{\Delta E}{kT} - \frac{\Delta\delta V}{V_s}\right)\right], \tag{6b}$$

and

$$K_2(V) = \exp\left(-\frac{\Delta E}{kT} - \frac{(\Delta\delta - 1)V}{V_s}\right), \tag{6c}$$

with $\Delta E = E_2 - E_1$ and $\Delta\delta = \delta_2 - \delta_1$

2. "Punch-Through" of Extracellular Blocker Molecules

A frequently applied experimental approach is that blocker molecules are applied extracellularly, while the intracellular concentrations remain low so that $[B_i] = 0$ can be assumed. If, in addition, a blocker molecule binds to the binding site in the channel pore with a Hill coefficient equal to 1 ($n_H = 1$, i.e., no cooperativity), Eq. (6) reduces to the Hill equation:

$$C(\infty) = \frac{I}{I_c}(V) = \frac{1}{1 + \left([B_o]/K_1(V)\right)}, \tag{7}$$

with K_1 given by Eq. (6b). Then, $K_1(V)$ can be interpreted as a voltage-dependent half-blocking concentration (K_D).

It can be shown that $K_1(V)$ may assume a minimum at a specific membrane potential V_0 with the consequence that at this voltage I/I_c is minimal so that at V_0 the blocking effect is maximal, independent from the applied extracellular concentration. This maximal block is reached at:

$$V_0 = -\frac{V_s}{\Delta\delta}\left(\frac{\Delta E}{kT} + \ln\frac{\delta_b}{\Delta\delta - \delta_b}\right) \tag{8}$$

As is obvious from Eq. (8), a minimum of K_1 at V_0 is only defined if $\Delta\delta - \delta_b > 0$. Put into words, this condition means that a maximum in

blocking efficacy is only reached if the distance between the energy barriers $\Delta\delta$ exceeds the distance of the binding site measured from the extracellular side. A maximum block at V_0 means that the block of positively charged molecules decreases if the membrane potential becomes more hyperpolarized than V_0. This effect has been termed "punch-through," as it can be interpreted as the electric field clearing a blocker molecule from the binding site and forcing it into the cytoplasm. From Eq. (8), it is clear that for positively charged blocker molecules and increased energy barrier height E_2 (i.e., increased ΔE), V_0 will shift to more negative potentials. This means that the "punch-through" is effectively resisted by increasing E_2 so that more blocker molecules will reside at the binding site. Inserting V_0 into the expression for K_1 [Eq. (6b)] gives:

$$K_1(V_0) = \exp\left(\frac{E_b - \Delta E \delta_b/\Delta\delta}{kT}\right) \Delta\delta \cdot (\Delta\delta - \delta_b)^{(\delta_b+\Delta\delta)/\Delta\delta} \cdot \delta_b^{-\delta_b/\Delta\delta} \qquad (9)$$

Apart from the dependence on the locations of energy barriers and binding site, given by the three most right-hand factors of Eq. (9), the first right-hand (exponential) factor indicates that the free energy of the binding site E_b is the most important parameter governing the half-blocking concentration K_1. If E_b is low (or negative), the molecules are strongly attracted to the binding site, in-line with Eq. (9), which shows that K_1 exponentially falls with E_b. A low K_1 means that even relatively low blocker concentrations will lead to a significant blocking effect [Eq. (7)].

3. Permeation Rate

The effective rate of entry or "punch-through" of blocker molecules at a specific membrane potential can be calculated from Eqs. (7) and (6b). In the absence of an intracellular concentration ($[B_i] = 0$), the entry rate R, that is the number of molecules entering per open channel per second, equals the blocked fraction CB times k_2:

$$R(V) = CB \cdot k_2 = [1 - C(\infty)]k_2 = \frac{k_2(V)}{1 + \left(K_1(V)/[B_o]\right)} \qquad (10)$$

If the block is of the "open channel" type, the total number of blocker molecules entering a cell per second through N_{ch} channels with an average open probability of p_o is given by:

$$N_{entry} = N_{ch} p_o R(V) = \frac{N_{ch} p_o k_2(V)}{1 + \left(K_1(V)/[B_o]\right)} \qquad (11)$$

Applying Eq. (11) to the OHC, an entry rate of 9000 DHS molecules per second per hair cell was calculated for a clinically relevant DHS concentration of 1 μM in the endolymph (further assuming 80 transducer channels per cell with a resting open probability of 0.3 due to the low endolymphatic Ca^{2+} concentration and an electrical driving force of -150 mV; Marcotti *et al.*, 2005). In contrast to the entry limiting effect of the strong binding ($E_b = -8.24kT$) and the intracellularly facing barrier having a considerable free energy ($E_2 = 15.84kT$), the extracellular barrier, because of its relatively low free energy ($E_1 = 10kT$), is easy to surmount by DHS. From the dynamics of DHS binding to the channel, a Ca^{2+}-dependent rate constant ($k_1 = 3.52 \times 10^8$ s^{-1} M^{-1}) could be determined under low Ca^{2+} (100 μM) conditions (Marcotti *et al.*, 2005). This relatively high value is indicative of an almost diffusion-limited influx of extracellular cations (Hille, 2001; Li and Aldrich, 2004).

4. Asymmetry in Blocking Potency of Extracellularly and Intracellularly Applied DHS

The salient features of the block by intracellular DHS reported by Marcotti *et al.* (2005; see Section V.A), namely the much lower potency of the block and block occurring at positive rather than negative membrane potentials can also be explained by the 2B1BS model. A reduction in efficacy in reaching the binding site from the intracellular side is evident from Eq. (6), which shows that the intracellular concentration is effectively multiplied by $K_2(V)$ in comparison to the extracellular concentration of the blocker molecules. The main contribution of $K_2(V)$ consists of the exponential factor $\exp(-\Delta E/kT)$, which amounts to about 8.8×10^{-3}, in-line with a reduced blocking effect of two to three orders of magnitude for intracellularly applied blockers. Another interesting feature of the 2B1BS model is that if both the rate constants related to the second barrier (k_2 and k_{-2}) are taken zero, it reduces to the Langmuir isothermal relation, describing the classical Woodhull blockage model, used by Kroese *et al.* (1989) to describe their measured blocking effects of aminoglycoside antibiotics. In the 2B1BS model, this corresponds to an infinite energy barrier height E_2, preventing the molecules to surmount it. This leads to a saturating constant block at strongly hyperpolarizing potentials, unlike the new observations of extracellularly applied DHS by Marcotti *et al.* (2005), which can only be described with a more complete permeant ($k_2 \neq 0$) version of the 2B1BS model (Section V.B.2). The observation that the block of intracellularly applied DHS occurs at positive potentials can be fitted by the 2B1BS model if a small value of $\Delta\delta$ is applied: $\Delta\delta \approx 0$. This can be interpreted as the two barriers coinciding at the intracellular side so that effectively no pathway to the extracellular space exists with the consequence that the drug cannot escape from its binding site

into the extracellular space. It is evident indeed from the measured block of intracellularly applied DHS (Marcotti *et al.*, 2005) that no signs of release at positive potentials are present like they are observed at negative potentials for extracellularly applied DHS. A physical asymmetry between extra- and intracellularly applied DHS may arise from the orientation that the molecules possess while their positive head groups are bound to the binding site. As will be described in more detail in Section VII, the pore most likely has a negatively charged binding site at about two-third of its length measured from the extracellular side, attracting the positive head group of a DHS molecule. When entering the pore from the intracellular side, the head group may bind to the same site, with the consequence that the DHS molecule is lined up with the pore so that its orientation is approximately at 180° with the geometry it has when entering from the extracellular side. In addition, part of the about 1.5-nm-long molecule could then still be in the cytoplasm, while the positive electrical field applied would not exert sufficient force to "punch" it out. This behavior would be consistent with DHS plugging the pore when applied from the inside and is therefore best described with the reduced version of the 2B1BS model that is equivalent to the classical Woodhull blockage model, as discussed above.

VI. TRANSDUCER CHANNEL BLOCK BY AMILORIDE AND ITS DERIVATIVES

A. Amiloride and Amiloride Derivatives as Permeant Transducer Channel Blockers: A Reinterpretation

The synthetic drug amiloride and related compounds find clinical application as potassium-sparing diuretics, thanks to their high-affinity blocking action (at submicromolar concentrations) on epithelial Na^+ channels in the distal and collecting tubules of the kidney (Kleyman and Cragoe, 1988). Amiloride has been found to reversibly inhibit the hair cell transducer current, but at higher concentrations (K_D around 50 μM; Jorgensen and Ohmori, 1988; Rüsch *et al.*, 1994), which is probably why no adverse effects of clinical treatment with amiloride on the auditory system have been reported. The drug has been used in early efforts to search for similarities of the hair cell transducer channel with other known ion channels and to gain information about the channel's gating mechanism. Amiloride and most of its derivatives are weak bases with a large fraction being protonated at physiological pH and hence carrying positive charges. With a molecular weight of 229.6 for the free base, amiloride is rather smaller than FM1-43 and the aminoglycosides and the maximum end-on diameter is about 0.6 nm

(Fig. 1). Studies using amiloride and benzamil (Fig. 1; a larger derivative of amiloride, with a molecular weight of 319.8, that blocks the transducer channel an order of magnitude more strongly) showed that, as for aminoglycosides, block is relieved at positive potentials. Furthermore, the drug-binding site can only be reached when the channel is open and the channel cannot close with the drug bound (Rüsch *et al*., 1994). The Hill coefficients for amiloride and related compounds were close to 2 (Rüsch *et al*., 1994), suggesting that two drug molecules are needed to block the channel, as for FM1-43 (Gale *et al*., 2001), but different from aminoglycosides for which one molecule suffices to block the channel (Kroese *et al*., 1989; Marcotti *et al*., 2005). Intracellularly applied amiloride at a high concentration of 1 mM did not appear to affect transducer currents (Rüsch *et al*., 1994).

At the time, the voltage dependence of the transducer channel block by amiloride was interpreted as being due to a conformational change on depolarization of the channel obscuring two amiloride-binding sites on the extracellular face of the channel, outside the electric field. At negative membrane potentials, the binding sites would be accessible and drug binding would result in an allosteric block of the channel (Rüsch *et al*., 1994; Kros, 1996). This "conformation model" of amiloride block was adopted to explain the incompleteness of the block at extreme negative potentials, a feature incompatible with the blocking mechanism that had been proposed for aminoglycosides by Kroese *et al*. (1989), namely that it would obstruct cation flow through the transducer channel by binding to a site within the pore reachable from the extracellular side only. A similar conformation model had already been applied to quantitatively explain amiloride block of mechanosensitive channels in frog oocytes (Lane *et al*., 1991), so this seemed to point to a satisfying similarity in the design of two different types of mechanoreceptor channel. Rüsch *et al*. (1994) considered amiloride binding inside the channel pore unlikely but not impossible: The incompleteness of the block at extreme negative potentials was also compatible with the drug molecules being punched through the channel to the intracellular side. This explanation was not pursued further, mainly because permeation of the transducer channel by large molecules was considered inconceivable.

The evidence that even larger molecules such as FM1-43 and DHS could permeate the transducer channel, and the various similarities between amiloride and aminoglycoside block that became apparent in the study of Marcotti *et al*. (2005) prompts a reexamination of amiloride block. The block by amiloride and benzamil can in fact be seen to be partially released at the largest negative potentials tested (see Figs. 3 and 4 in Rüsch *et al*., 1994). Consequently, their data can be better fitted with the 2B1BS model (Section V.B) than with the original conformation model, which does not accommodate the reduction of the block at hyperpolarized potentials seen in

the data (Fig. 5). The fitting parameters are qualitatively similar to those for DHS, but with the binding site positioned about halfway through the pore, less difference in the height and distance of the two energy barriers, and a stronger attraction to the binding site in the pore. Most likely this reflects differences in size and position of the electrical charges between the amiloride and benzamil molecules on the one hand and DHS on the other. The finding that amiloride, like the aminoglycosides, can alter the mechanics of the transducer channel corroborates the idea that both act on the channel in essentially the same way (Denk *et al.*, 1992; Wiersinga-Post and Van Netten, 1998). Novel testable predictions from the new interpretation of the interaction of amiloride with the hair cell transducer channel include that the positively charged rather than the neutral form blocks the channel, that lowering extracellular Ca^{2+} will increase the potency of the block, and that at higher concentrations than those tested before, it will block transduction from the intracellular side. It remains to be seen whether amiloride turns out to be a permeant blocker of other mechanoreceptors, including those of frog oocytes.

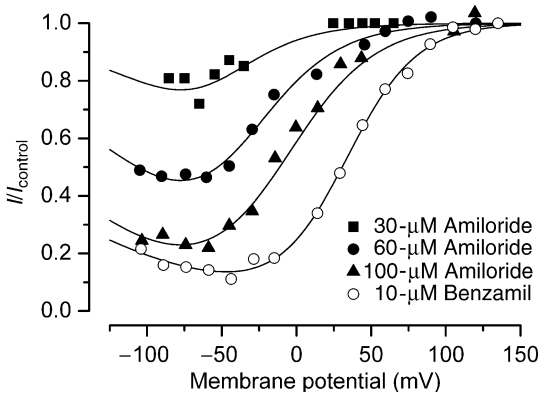

FIGURE 5 Mechanoelectrical transducer currents in mouse OHCs blocked by extracellularly applied amiloride and benzamil, depicted as a fraction of control currents (data are from Fig. 4 in Rüsch *et al.*, 1994, with permission). The voltage dependence of the block, in the presence of 1.3-mM extracellular Ca^{2+}, is shown for three concentrations of amiloride (30, 60, and 100 μM) and one concentration of benzamil (10 μM). Continuous lines were calculated with the 2B1BS model [Section V.B.1; Eq. (6)], in contrast with an earlier interpretation of the same data in terms of a conformation model of blockage (Rüsch *et al.*, 1994). Parameters used in the model are the same for all concentrations shown for amiloride: $\Delta E = E_2 - E_1 = 3.2kT$; $\Delta\delta = \delta_2 - \delta_1 = 0.66$; $E_b = -18.1kT$; $\delta_b = 0.44$, $n_H = 2$, and $z = 2$. For benzamil, the parameters used were $\Delta E = E_2 - E_1 = 1.37kT$; $\Delta\delta = \delta_2 - \delta_1 = 0.71$; $E_b = -24.4kT$; $\delta_b = 0.55$, $n_H = 2$, and $z = 2$. The better fits to the data with the 2B1BS model than those obtained with the conformational model indicates that also amiloride and benzamil are permeant blockers of the mechanoelectrical transducer channel.

B. Structure-Activity Sequences for Amiloride and Its Derivatives

Because of their clinical application and hence commercial interest, about a thousand bulkier compounds related to amiloride have been synthesized (Kleyman and Cragoe, 1988). This allows for a comparison as to how the addition of various side chains at different positions of the molecule affect the K_D for its different targets. For example, the so-called structure-activity sequence is very different between the kidney epithelial Na^+ channel and the hair cell transducer channel (Rüsch *et al.*, 1994). Of the various ion channels and transporters that can be blocked by amiloride and its analogues, only the mechanosensitive channel of frog oocytes had a similar sequence to that of the hair cell transducer channel (Lane *et al.*, 1992; Rüsch *et al.*, 1994). It would be interesting to extend this analysis to mechanosensitive channels in other sensory systems to seek for common properties.

VII. CONCLUSIONS

The results discussed in the preceding sections may be summarized by constructing a putative geometrical model of the transducer channel with a specific charge distribution lining the pore (Fig. 6). The interactions of the channel with the alkali metal cations, divalent cations (in particular Ca^{2+}), the permeant cationic blocker molecules discussed in this chapter as well as other polycationic blocker molecules that have been investigated (Farris *et al.*, 2004), all support the conclusion that at about halfway the pore a negative charge distribution forms a binding site. A binding site's location that is obtained from fitting barrier models (including the 2B1BS model) is usually estimated in terms of electrical distances. These cannot directly be translated into physical distances along the pore. The differences in the binding site's apparent position as obtained from fitting the 2B1BS model to DHS ($\delta_b = 0.79$), amiloride ($\delta_b = 0.44$), and benzamil ($\delta_b = 0.55$) could be due to differences in the blockers and may very well indicate the presence of a single dominating negatively charged region in the pore. These permeant molecules are structurally different so that, when bound, the positive groups responsible for binding are located at different distances from the negative charges. This would, under the assumption of equal valence (+2), lead to significantly different binding energies E_b as supported by the model fits (DHS $= -8.27kT$; amiloride $= -18.1.1kT$; benzamil $= -24.4kT$). The Eisenman sequence established for the transducer channel suggests this negatively charged region to be the selectivity filter. On the basis of the length of the nonblocking FM3-25 molecule, the negative binding site was estimated to be located at about 2 nm inside the pore, measured from the extracellular side,

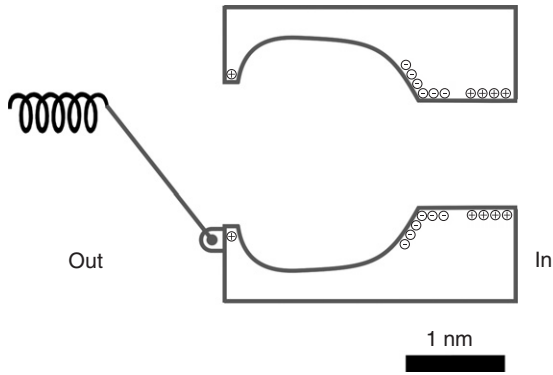

FIGURE 6 Putative model of the hair cell transducer channel pore. The charge distribution and dimensions depicted are based on a combination of results from fitting the 2B1BS model to DHS blocking data and results on other permeant blockers and other data. Positive charges reflect energy barriers, while negative charges indicate a binding site, most likely related to the selectivity filter (Section III). The large vestibule on the extracellular side (Out) must reach at least 1.8 nm into the pore as to prevent FM3-25 molecules to reach the negatively charged binding site depicted at about 2 nm from the extracellular side (Section IV.A). The narrowest part of the pore, facing the intracellular side (In), must have at least an effective diameter of 1 nm in order to accommodate permeation of the large aminoglycoside molecules into the cytoplasm (Farris *et al*., 2004, who estimate its narrowest diameter as 1.25 nm). The total length of the channel pore is estimated to be ~3 nm. The transducer channel's gate, engaged by the gating spring, is schematically depicted at the extracellular side. Gating of the transducer channel, however, is most likely related to conformational changes of the channel that effectively closes the pore to ions and permeant molecules, some of which (e.g., Ca^{2+} and FM1-43) may become trapped inside the vestibule.

while the total membrane spanning pore length was approximated by about 3 nm (Farris *et al.*, 2004). The two barriers assumed in the 2B1BS model can for all three types of molecules described with the 2B1BS model be associated with positive free energies and are thus indicated with positive charges (Fig. 6). Also, for these three types of molecules, the barrier energy at the intracellular side (E_2) exceeds that of the extracellularly facing one (E_1) with one to several times kT. The lower energy of the extracellular barrier is associated in the case of DHS with a second-order (i.e., concentration dependent) rate constant that suggests a high, extracellular Ca^{2+}-dependent influx of extracellular cations that is almost diffusion limited. This points to a relatively large vestibule, as depicted in Fig. 6. The vestibule should at least be large enough to accommodate two FM1-43 molecules (maximum end-on diameter 0.78 nm and length about 2.2 nm) that can be trapped if the channel's gate closes. The gate is schematically indicated as an extracellularly located element. Gating of the transducer channel, however, is most likely related to conformational changes of the vestibular region of the pore of the

channel that effectively open and close the pore to ions and permeant molecules.

Taken together, a functional channel pore model of the transducer channel is emerging that facilitates the entry into the hair cell of relatively large extracellular molecules that all seem to interact or compete with Ca^{2+}. The physiological significance of this design is that it is likely to be important for the extremely large single-channel conductance of the transducer channel: a range of 150–300 pS has been reported for endolymphatic (i.e., low) extracellular Ca^{2+} concentrations (Ricci *et al.*, 2003). These large conductances are similar to those reported for large-conductance Ca^{2+}-activated K^+ channels (BK channels) in which a large vestibule (but placed on the intracellular side of the channel) lined with a ring of negative charges is proposed to promote a large single-channel conductance by allowing near-diffusion limited access of intracellular K^+ ions to the selectivity filter (Brelidze *et al.*, 2003; Li and Aldrich, 2004; Brelidze and Magleby, 2005). The single-channel conductance of the transducer channel is tonotopically organized in that it gradually and systematically changes along the cochlea, with high-frequency hair cells having the largest conductance (Ricci *et al.*, 2003). Future work is likely to establish the molecular identity of the channel, which can then be investigated with several permeant molecules that have given us already some insights into the channel pore. For example, it would be interesting to test whether the tonotopic gradient in transducer channel conductance is due to a systematic change in the dimensions or number of negative charges in the vestibule.

Acknowledgments

Supported by the Netherlands Organisation for Scientific Research (S.M.v.N) and the MRC (C.J.K.). The authors thank Dr. Cécil J. W. Meulenberg for his comments on an early version of this chapter and his help with the preparation of Fig. 1.

References

Betz, W. J., and Bewick, G. S. (1992). Optical analysis of synaptic vesicle recycling at the frog neuromuscular junction. *Science* **255,** 200–203.

Betz, W. J., Mao, F., and Bewick, G. S. (1992). Activity dependent fluorescent staining and destaining of living vertebrate motor nerve terminals. *J. Neurosci.* **12,** 363–375.

Brelidze, T. I., and Magleby, K. L. (2005). Probing the geometry of the inner vestibule of BK channels with sugars. *J. Gen. Physiol.* **126,** 105–121.

Brelidze, T. I., Niu, X., and Magleby, K. L. (2003). A ring of eight conserved negatively charged amino acids doubles the conductance of BK channels and prevents inward rectification. *Proc. Natl. Acad. Sci. USA* **100,** 9017–9022.

Cochilla, A. J., Angelson, J. K., and Betz, W. J. (1999). Monitoring secretory membrane with FM1-43 fluorescence. *Ann. Rev. Neurosci.* **22,** 1–10.

Corey, D. P. (2006). What is the hair cell transduction channel? *J. Physiol.* **576,** 23–28.

Crawford, A. C., Evans, M. G., and Fettiplace, R. (1991). The actions of calcium on the mechano-electrical transducer current of turtle hair cells. *J. Physiol.* **434,** 369–398.

Denk, W., Keolian, R. M., and Webb, W. W. (1992). Mechanical response of frog saccular hair bundles to the aminoglycoside block of mechanoelectrical transduction. *J. Neurophysiol.* **68,** 927–932.

Farris, H. E., LeBlanc, C. L., Goswami, J., and Ricci, A. J. (2004). Probing the pore of the auditory hair cell mechanotransducer channel in turtle. *J. Physiol.* **558,** 769–792.

Fettiplace, R., and Ricci, A. J. (2006). Mechanoelectrical transduction in auditory hair cells. *In* "Vertebrate Hair Cells" (R. A. Eatock, R. R. Fay, and A. N. Popper, eds.), pp. 154–203. Springer Science and Business Media, New York.

Forge, A., and Schacht, J. (2000). Aminoglycoside antibiotics. *Audiol. Neurootol.* **5,** 3–22.

Gale, J. E., Marcotti, W., Kennedy, H. J., Kros, C. J., and Richardson, G. P. (2001). FM1-43 dye behaves as a permeant blocker of the hair-cell's mechanotransducer channel. *J. Neurosci.* **21,** 7013–7025.

Géléoc, G. S. G., and Holt, J. R. (2003). Developmental acquisition of sensory transduction in hair cells of the mouse inner ear. *Nat. Neurosci.* **6,** 1019–1020.

He, D. Z. Z., Jia, S., and Dallos, P. (2004). Mechanoelectrical transduction of adult outer hair cells studied in a gerbil hemicochlea. *Nature* **429,** 766–770.

Hiel, H., Erre, J. P., Aurousseau, C., Bouali, R., Dulon, D., and Aran, J. M. (1993). Gentamicin uptake by cochlear hair cells precedes hearing impairment during chronic treatment. *Audiology* **32,** 78–87.

Hille, B. (2001). "Ion Channels of Excitable Membranes," 3rd ed. Sinauer Associates, Sunderland, MA.

Howard, G., and Hudspeth, A. J. (1988). Compliance of the hair bundle associated with gating of mechanoelectrical transduction channels in the bullfrog's saccular hair cell. *Neuron* **1,** 189–199.

Howard, J., Roberts, W. M., and Hudspeth, A. J. (1988). Mechanoelectrical transduction by hair cells. *Ann. Rev. Biophys. Biophys. Chem.* **17,** 99–124.

Jorgensen, F., and Kroese, A. B. A. (1995). Calcium selectivity of the transducer channel in hair cells of the frog sacculus. *Acta Physiol. Scand.* **155,** 363–376.

Jorgensen, F., and Ohmori, H. (1988). Amiloride blocks the mechano-electrical transduction channel of hair cells in the chick. *J. Physiol.* **403,** 577–588.

Kleyman, T. R., and Cragoe, E. J., Jr. (1988). Amiloride and its analogs as tools in the study of ion transport. *J. Membrane Biol.* **105,** 1–21.

Konishi, T. (1979). Effects of local application of ototoxic antibiotics on cochlear potentials in guinea pigs. *Acta Otolaryngol.* **88,** 41–46.

Kroese, A. B. A., Das, A., and Hudspeth, A. J. (1989). Blockage of the transduction channels of hair cells in the bullfrog's sacculus by aminoglycoside antibiotics. *Hear. Res.* **37,** 203–218.

Kros, C. J. (1996). Physiology of mammalian cochlear hair cells. *In* "The Cochlea" (P. Dallos, A. N. Popper, and R. R. Fay, eds.), pp. 318–385. Springer-Verlag, New York.

Kros, C. J., Rüsch, A., and Richardson, G. P. (1992). Mechano-electrical transducer currents in hair cells of the cultured neonatal mouse cochlea. *Proc. R. Soc. Lond. B* **249,** 185–193.

Kros, C. J., Marcotti, W., van Netten, S. M., Self, T. J., Libby, R. T., Brown, S. D. M., Richardson, G. P., and Steel, K. P. (2002). Reduced climbing and increased slipping adaptation in cochlear hair cells of mice with *Myo7a* mutations. *Nat. Neurosci.* **5,** 41–47.

Kros, C., Marcotti, W., and van Netten, S. (2006). Aminoglycoside ototoxicity depends on drug entry through the hair-cell transducer channels. *Assoc. Res. Otolaryngol. Abs.*: p. 85.

Lane, J. W., McBride, D. W., Jr., and Hamill, O. P. (1991). Amiloride block of the mechanosensitive cation channel in *Xenopus* oocytes. *J. Physiol.* **441,** 347–366.

Lane, J. W., McBride, D. W., Jr., and Hamill, O. P. (1992). Structure-activity relations of amiloride and its analogues in blocking the mechanosensitive channel in *Xenopus* oocytes. *Br. J. Pharmacol.* **106,** 283–286.

Li, W., and Aldrich, R. W. (2004). Unique inner pore properties of BK channels revealed by quaternary ammonium block. *J. Gen. Physiol.* **124,** 43–57.

Marcotti, W., van Netten, S. M., and Kros, C. J. (2005). The aminoglycoside antibiotic dihydrostreptomycin rapidly enters hair cells through the mechano-electrical transducer channels. *J. Physiol.* **567,** 505–521.

Matsuura, S., Ikeda, K., and Furukawa, T. (1971). Effects of streptomycin, kanamycin, quinine, and other drugs on the microphonic potentials of goldfish sacculus. *Jpn. J. Physiol.* **21,** 579–590.

Meyers, J. R., MacDonald, R. B., Duggan, A., Lenzi, D., Standaert, D. G., Corwin, J. T., and Corey, D. P. (2003). Lighting up the senses: FM1-43 loading of sensory cells through nonselective ion channels. *J. Neurosci.* **23,** 4054–4065.

Nishikawa, S., and Sasaki, F. (1996). Internalization of styryl dye FM1-43 in the hair cells of lateral line organs in *Xenopus* larvae. *J. Histochem. Cytochem.* **44,** 733–741.

Ohmori, H. (1985). Mechano-electrical transduction currents in isolated vestibular hair cells of the chick. *J. Physiol.* **359,** 189–217.

Ricci, A. J. (2002). Differences in mechano-transducer channel kinetics underlie tonotopic distribution of fast adaptation in auditory hair cells. *J. Neurophysiol.* **87,** 1738–1748.

Ricci, A. J., and Fettiplace, R. (1998). Calcium permeation of the turtle hair cell mechano-transducer channel and its relation to the composition of endolymph. *J. Physiol.* **506,** 159–173.

Ricci, A. J., Crawford, A. C., and Fettiplace, R. (2003). Tonotopic variation in the conductance of the hair cell mechanotransducer channel. *Neuron* **40,** 983–990.

Rüsch, A., Kros, C. J., and Richardson, G. P. (1994). Block by amiloride and its derivatives of mechano-electrical transduction in outer hair cells of mouse cochlear cultures. *J. Physiol.* **474,** 75–86.

Schacht, J. (1986). Molecular mechanisms of drug-induced hearing loss. *Hear. Res.* **22,** 297–304.

Seiler, C., and Nicolson, T. (1999). Defective calmodulin-dependent rapid apical endocytosis in zebrafish sensory hair cell mutants. *J. Neurobiol.* **41,** 424–433.

Si, F., Brodie, H., Gillespie, P. G., Vazquez, A. E., and Yamoah, E. N. (2003). Developmental assembly of transduction apparatus in chick basilar papilla. *J. Neurosci.* **23,** 10815–10826.

Taura, A., Kojima, K., Ito, J., and Ohmori, H. (2006). Recovery of hair cell function after damage induced by gentamicin in organ culture of rat vestibular maculae. *Brain Res.* **1098,** 33–48.

Wersäll, J., Bjorkroth, B., Flock, A., and Lundquist, P. G. (1973). Experiments on ototoxic effects of antibiotics. *Adv. Otorhinolaryngol.* **20,** 14–41.

Wiersinga-Post, J. E., and van Netten, S. M. (1998). Amiloride causes changes in the mechanical properties of hair cell bundles in the fish lateral line similar to those induced by dihydrostreptomycin. *Proc. R. Soc. Lond. B* **265,** 615–623.

Woodhull, A. M. (1973). Ionic blockage of sodium channels in nerve. *J. Gen. Physiol.* **61,** 687–708.

Zhao, Y.-D., Yamoah, E. N., and Gillespie, P. G. (1996). Regeneration of broken tip links and restoration of mechanical transduction in hair cells. *Proc. Natl. Acad. Sci. USA* **93,** 15469–15474.